Forschung im Ingenieurwesen (2024)88:37
https://doi.org/10.1007/s10010-024-00759-x

ORIGINALARBEITEN/ORIGINALS

Surface roughness measurement in the notch area for estimating dynamic component load bearing capacity

Nils Becker[1] · **Paul Tunsch**[1] · **Carsten Ulrich**[1] · **Berthold Schlecht**[1]

Received: 13 November 2023 / Accepted: 20 August 2024

Abstract

The surface of a part can have an essential influence on its dynamic load bearing capacity as grooves and scratches act as more or less significant imperfections or additional micro-notches, depending on the interpretation. In order to accurately predict the fatigue strength, detailed knowledge of the surface structure in critical areas is essential but cannot always be established due to geometric constraints. To overcome these restrictions, a method utilizing impressions and a laser scanning microscope to take surface topography measurements in critical notch areas is used in this work. It enables precise and reproducible measurements to be taken. The method is used to conduct surface roughness measurements on fatigue strength specimens made of four different materials. Several roughness influence factors are calculated based on the results and their influence on the result of a recalculation using a fatigue strength assessment is shown as example. The calculated fatigue limit is compared against experimental results. The comparison shows significant scatter in prediction accuracy and no optimal surface influence factor can be recommended so far. It has to be noted that only a small sample of specimens, which were not designed for researching surface roughness influence in particular, were available for this work. The effects of roughness in the notch may not be completely captured by the available roughness influence factors. Furthermore, issues arise in the correct implementation of stress concentration factor based roughness influence factors. Further research is required to provide a more comprehensive understanding of the effects of surface roughness on the fatigue limit.

✉ Nils Becker
nils.becker@tu-dresden.de

Paul Tunsch
paul.tunsch@tu-dresden.de

Carsten Ulrich
carsten.ulrich@tu-dresden.de

Berthold Schlecht
berthold.schlecht@tu-dresden.de

[1] Professur für Maschinenelemente, Technische Universität Dresden, 01062 Dresden, Germany

Published online: 20 September 2024

Rauheitsmessung im Kerbbereich zur Abschätzung der dynamischen Bauteiltragfähigkeit

Zusammenfassung

Die Oberfläche eines Bauteils kann einen wesentlichen Einfluss auf seine dynamische Tragfähigkeit haben, da Rillen und Kratzer je nach Interpretation als mehr oder weniger große Unvollkommenheiten oder zusätzliche Mikrokerben wirken. Für eine genaue Vorhersage der Ermüdungsfestigkeit ist eine detaillierte Kenntnis der Oberflächenstruktur in kritischen Bereichen unerlässlich, die jedoch aufgrund geometrischer Beschränkungen nicht immer erlangt werden kann. Um diese Einschränkungen zu überwinden, wird in dieser Arbeit eine Methode verwendet, bei der Abdrücke und ein Laser-Scanning-Mikroskop zur Messung der Oberflächentopografie in kritischen Kerbbereichen eingesetzt werden. Sie ermöglicht präzise und reproduzierbare Messungen. Mit dieser Methode werden Oberflächenrauheitsmessungen an Dauerfestigkeitsproben aus vier verschiedenen Werkstoffen durchgeführt. Anhand der Ergebnisse werden verschiedene Rauheitseinflussfaktoren berechnet und deren Einfluss auf das Ergebnis einer Nachrechnung mit einer Dauerfestigkeitsbewertung beispielhaft dargestellt. Die berechnete Dauerfestigkeit wird mit experimentellen Ergebnissen verglichen. Der Vergleich zeigt erhebliche Streuungen in der Vorhersagegenauigkeit, es kann bisher kein optimaler Oberflächeneinflussfaktor empfohlen werden. Es ist anzumerken, dass für diese Arbeit nur eine kleine Stichprobe von Proben zur Verfügung stand, die nicht speziell für die Untersuchung des Einflusses der Oberflächenrauheit konzipiert waren. Die Rauheitseffekte in der Kerbe werden möglicherweise nicht vollständig von den verfügbaren Rauheitseinflussfaktoren erfasst. Darüber hinaus ergeben sich Probleme bei der korrekten Anwendung von Rauheitsfaktoren, die auf Spannungskonzentrationsfaktoren für Mikrokerben basieren. Weitere Untersuchungen sind erforderlich, um ein umfassenderes Verständnis der Auswirkungen der Oberflächenrauheit auf die Dauerfestigkeit zu erlangen.

1 Introduction

Fatigue strength is an important factor for the design of a drivetrain, as parts have to endure a high number of load cycles. Therefore, one of the main goals in drivetrain design is a prediction that is as accurate as possible for the fatigue strength. While undersizing of machine elements can have dramatic consequences like destruction of the whole system, oversizing leads to unnecessary weight and additional expense in material. As shafts are one of the most important machine elements in drivetrains, they are the focus of this work.

Fatigue strength prediction of shafts and axles is typically based on standards like DIN 743 [1] or guidelines like Analytical Strength Assessment [2]. Both provide nominal stress approaches, which are easy to use for the dimensioning of shafts. In these approaches, different influences on the fatigue strength of a part are accounted for by influence factors that modify the material strength according to shape and state of the part. As research in drive technology progresses, a better understanding of effects on component strength develops and better estimation factors can be implemented into standards and guidelines. While roughness is an important influence on fatigue strength, the calculation of this influence still relies on almost 70 year old research [3].

One of the main issues in researching the roughness influence on fatigue strength is the geometric shape of the critical notches. As shafts usually break at notches, it is desirable to measure the roughness directly in the notch. Common measuring techniques are not able to measure at this location due to geometric constraints. Becker et al. [4] described a method using impressions made of dental impression material to enable roughness measurement in notches through a negative of the surface. This method can be used to take roughness measurements in notches of shafts and further investigate the roughness influence on fatigue strength. In this work, the shown method is further refined in order to increase reproducibility and accuracy of the measurements. Measurements are taken on fatigue strength specimens made of four materials and surface texture parameters as well as roughness influence factors are calculated. The roughness influence factors are implemented into the FKM-guideline [2] and calculated fatigue strength is compared against experimental results.

2 Methodology

2.1 Development of the evaluation process

Specimens for this work were taken from a current research project investigating the effects of mechanical surface treatments on the fatigue strength. Specimen geometry is shown in Fig. 1, all specimens possess a shaft shoulder with nominal diameters $D = 30\,mm$, $d = 14\,mm$ and a notch radius of $r = 0.4\,mm$.

To achieve a high reproducibility of the measurements, special impression casts were constructed and 3D-printed. Two different kinds of cast, shown in Fig. 2, were used. Impressions taken with the cast on the left of Fig. 2 can be used to examine roughness directly in the notch, as the

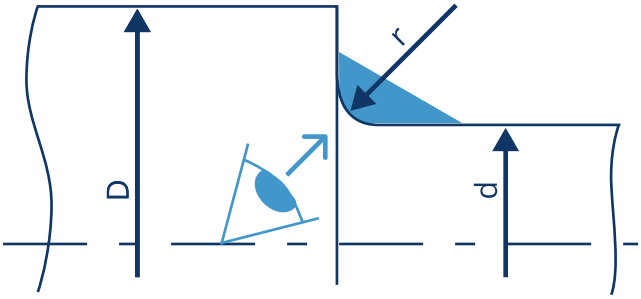

Fig. 1 Geometry of specimen notches

Table 1 Setup of the laser scanning microscope

Microscope	Zeiss LSM 5 Exciter
Objective	Zeiss LD EC Epiplan NEOFLUAR
Objective magnification	100 x
Total magnification	1000 x
Numerical aperture	0.75
Laser wavelength	405 nm
Laser power (impressions)	25 mW (100%)
z-step	0.69 µm
x-step, y-step	0.23 µm

maximum stress location is parallel to the x-y-plane of the microscope. The cast shown on the right of Fig. 2 can be used to take reference measurements on the cylinder surface of the specimens. The casts are connected to a second half, which allows for secure positioning of the specimen with connecting pins. Afterwards the impression cavity can be filled with impression material through a dedicated canal. After curing, the cast can be removed from the specimen and the impression can be removed from the cast.

Measurements of surface topography were conducted using a laser scanning microscope. The setup of the microscope is summarized in Table 1. Becker et al. [4] used the same setup with a much smaller z-step. The z-step refers to the height distance between two images. Selecting a larger z-step reduces the number of images required to scan a given height. The necessary z-step was reviewed in order to increase measurement speed. Based on the optical section thickness [5] and the Nyquist-Shannon sampling theorem, it was determined that a z-step of 0.69 µm is adequate for detecting the specimen surface without any loss of information. This increase in z-step results in nearly sevenfold faster measurement times. Consequently, surface scans are conducted for all measurements within a reasonable time frame. Surface defects and artefacts can be more effortlessly detected in a surface scan than in a profile scan. The z-resolution was enhanced by a factor of ten by means of spline interpolation resulting in a resolution sufficient to detect surface features.

Multiple processing steps must be applied after electromagnetic surface detection to determine the surface texture parameters that are necessary for calculating the surface's influence on the fatigue limit. Noise suppression, inverting of the coordinates and subtraction of a polynomial background are performed as described in [4]. As a means of noise suppression, all profile points with an intensity maximum less than 20% above the average noise are removed and replaced with linear interpolation between neighboring profile points. This technique helps to reduce measurement artifacts, such as those found on edges. Additionally, by inverting the z-coordinates, the impression's surface can be virtually transformed into the shape of the original component. To enhance the recognition of surface details and facilitate profile processing and filtering, the original image undergoes a subtraction process where the nominal shape of the notch is removed. This is achieved by fitting a polynomial surface of degree 2 along the notch radius and degree 1 transverse to it to the original image, which is then subtracted from the original image.

Profiles are obtained from the surface scan since all surface influence factors used in this study depend on profile-based values. Surface texture parameters R_t, R_z and R_v are calculated according to ISO 21920 [6] and used to calculate the roughness influence factors in this work. Calculation of R_a, R_p, R_{sm} and R_{mc} is also implemented but was not used to calculate roughness influence factors. The profiles are filtered according to setting class Sc1 as no profiles suitable for a higher setting class could be taken in the notch due to technical restrictions. Setting class Sc1 is normally used for much smaller surface texture parameter ranges and leads to an underestimation of surface texture parameters in this case. To assess this effect, the corresponding P-values based on the unfiltered surface profile are calculated too. The parameters for surface texture roughness calculation are determined by calculating the mean value of the sur-

Fig. 2 Impression casts

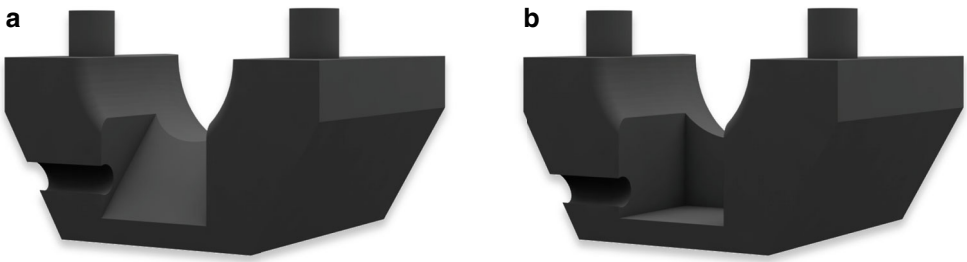

Table 2 Overview of roughness influence factors considered for this work

Roughness influence factor	Equation	
FKM	$K_{F\sigma} = 1 - a_{R,\sigma} \cdot \log(R_z) \cdot \log\left(\frac{2 \cdot R_m}{R_{m,N,\min}}\right)$	(1)
Hück	$K_{F\sigma} = 1 - 0{,}22 \cdot \log(R_z)^{0{,}64} \cdot \log(R_m) + 0{,}45 \cdot \log(R_z)^{0{,}53}$	(2)
Liu	$K_{F\sigma} = \frac{1}{1+\left[(K_{O,\sigma}-1)^{-2{,}5}+\left(\sqrt{1+\frac{R_{\text{eff}}}{\Delta_0}}-1\right)^{-2{,}5}\right]^{-0{,}4}}$	(3)
Approaches using stress concentration factors		
Liu	$K_{O,\sigma} = 1 + \left(2 - \frac{b}{B}\right) \cdot \sqrt{\frac{t}{\rho}}$	(4)
Peterson	$K_{O,\sigma} = 1 + 2\sqrt{\frac{t}{\rho}}$	(5)
Neuber	$K_{O,\sigma} = 1 + 2\sqrt{\lambda \frac{R_z}{\rho}}$	(6)
Arola-Ramulu	$K_{O,\sigma} = 1 + 2\left(\frac{R_a}{\rho}\right)\left(\frac{R_y}{R_z}\right)$	(7)

face texture parameters for all profiles in a single surface scan. The surface texture parameter calculation results are cross-checked with the reference software RPTB to ensure accuracy [7].

In addition to examining roughness influence factors based on surface texture parameters, those based on notch factors are also investigated. To calculate stress concentration factors for surface notches, the notch radius has to be determined. The utilized method is based on work of Arola and Williams [8], which use a graphical radius gage to estimate radii at least at three critical valleys on a depiction of the profile with an aspect ratio of 1:1. In this work, minima of the profile are detected automatically. Afterwards, a circle is fitted into each minimum using all points within 1 µm distance to the minimum. Circles with a center below the surface profile are discarded. The smallest radius of all remaining circles is used to calculate roughness influence, as this results in the highest roughness influence factors, see equations in Table 2. The workflow to process the raw LSM intensity data into roughness influence factors for fatigue is summarized in Fig. 3.

2.2 Integration into the fatigue limit assessment

Several approaches to predict surface influence on the fatigue limit are implemented to compare prediction quality. They can be categorized into empirical factors and notch factor based approaches.

The empirical factor used in the standard DIN 743-2 [9] and FKM guideline [2] is based on the work of Siebel and

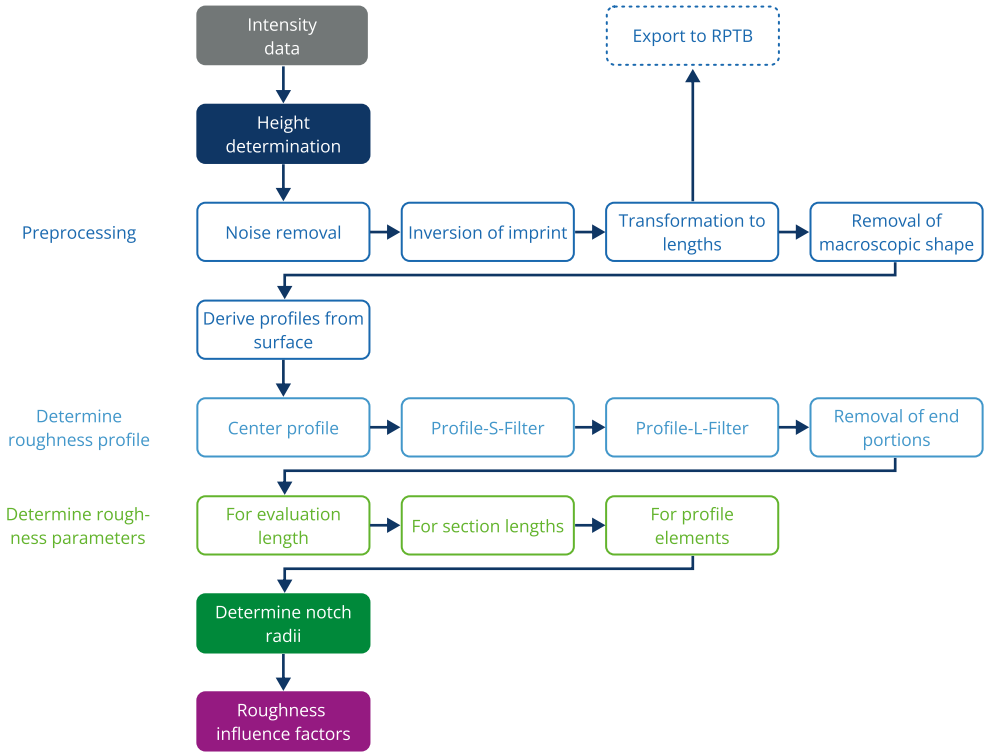

Fig. 3 Workflow to determine surface parameters from LSM data

Gaier [3] and is calculated according to Eq. 1. It uses the maximum height R_z to consider surface roughness. Material dependent roughness sensitivity is implemented through the tensile strength R_m. The same parameters are used in the roughness factor according to Hück [10, 11], see Eq. 2.

Another empirical factor is developed by Liu [12], see Eq. 3. It applies fracture-mechanical material characteristics and considers surface roughness in terms of an efficient roughness value R_{eff}. The effective roughness R_{eff} is set to $R_{eff} = R_t/3$ in this work. The geometry of surface micro-notches finds further consideration through the notch factor $K_{O,\sigma}$. Based on evaluations of the surface profiles analyzed in this work, it can be concluded that the distance between two surface notches equals their width, hence b/B can be set to 1.

Other approaches consider the effects of surface roughness solely via a surface stress concentration factor. Thereby, each roughness valley is regarded as a single shallow notch. In this case, stress concentration can be calculated using Eq. 5 according to Peterson [13]. In this method, only geometric parameters notch depth t and notch radius ϱ are considered.

To take into account the relief effect of several adjacent notches, Neuber [14] proposed a simplified relationship as given in Eq. 6. It removes the need of the hard-to-measure notch depth and replaces it by the maximum height R_z.

This was further elaborated on by Arola and Ramulu [15], resulting in Eq. 7. This stress concentration factor was developed using an ideal sinusoidal profile and is able to consider waviness components through the ratio of total height R_y to maximum height R_z.

2.3 Issues concerning stress concentration factor based roughness influence factors

One of the main advantages of micro-notch-based approaches in terms of stress concentration factors over the merely empirical approaches is that they can be captured statistically in a very accurate way. Vetter, for example, makes consistent use of this to implement a probabilistic failure model of the component surface in his load-bearing capacity analysis [16, 17]. In addition, the consideration of a micro-notch effect, which is based only on the micro geometry and acts simply in addition to the macroscopic notch, offers the prospect of a mechanically very precisely describable effect. However, this supposed mechanical accuracy quickly reaches its limits with regard to several issues. Steels have a highly inhomogeneous and anisotropic microstructure. Due to the statistical K_t-K_f ratio (defect-based size effect), a certain influence of randomly distributed defects with statistically distributed damage potential can be taken into account based on the weakest link principle [18, 19]. Nevertheless, all parameters used in classical fatigue strength assessments rely on the assumption of a sufficiently large highly stressed area with a sufficiently large number of grains in it. This applies to the equivalent stress hypotheses, the material fatigue strength itself and many further details. The analytical or numerical calculation of notch stress states with homogeneous or continuously variable material models therefore only makes sense as long as the notch is large enough in relation to the microstructure. Figure 4 shows a surface profile measured using the method presented above with a nominal notch radius of 0.4 mm. After taking the impression, a lengthwise micrograph was taken and the measured roughness profile was superimposed to scale. As the picture clearly demonstrates, the assumption of homogeneous material properties and thus the calculation of micro stress concentration factors or supposed micro-notch stress states in the roughness profile seems essentially unjustified.

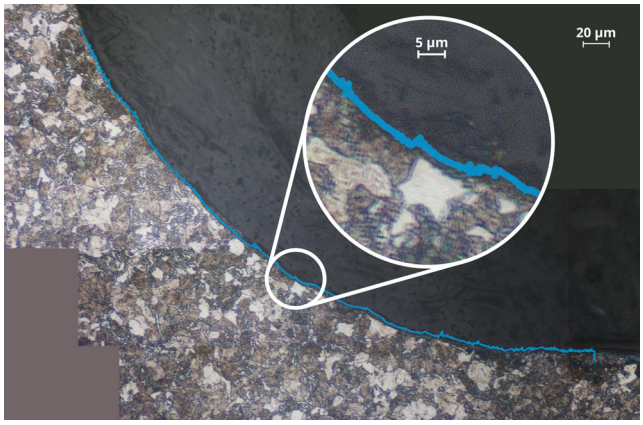

Fig. 4 Micrograph with impression-measured roughness profile superimposed to scale [20]

In addition to the fundamental issue concerning the microstructure described above, there are also simple practical questions regarding the implementation of micro-notch effects into established fatigue strength assessments while maintaining mechanical consistency. In particular, the superposition with the macroscopic notch is highly questionable if the deformation-mechanical and statistical K_t-K_f ratio are still to be used in their classical sense. Due to these uncertainties and because the present study initially aims to make a basic comparison against the background of established guidelines and standards, the stress concentration factor based parameters are not considered in the following.

3 Results

To evaluate the accuracy of the surface influence factors, four steel specimens were used. Specimen 1 is made of quenched and tempered C45. Quenched and tempered 42CrMo4 with an unusually high strength is used for

Table 3 Properties of the specimens used

	Specimen 1 C45 + QT	Specimen 2 42CrMo4 + QT	Specimen 3 C45 + *N*	Specimen 4 EN-GJS-600-3
Tensile strength R_m [MPa]	780	1572	618	626
Young's modulus E [GPa]	210.7	207.7	210.0	172.2
Experimental fatigue limit rotary bending σ_{bWK} [MPa]	164	278	136	175
Notch diameter D [mm]	29.9874	29.9847	29.9893	29.9904
Notch diameter d [mm]	14.0042	14.0132	14.0034	14.0039
Notch radius r [mm]	0.4142	0.4131	0.404	0.4232

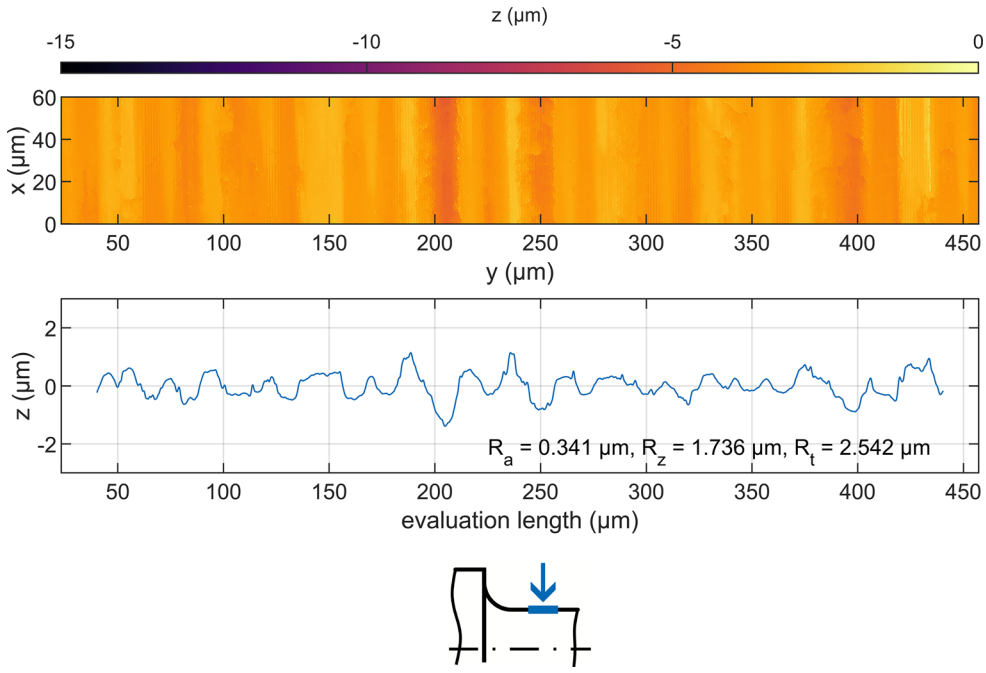

Fig. 5 Surface scan and filtered roughness profile on the cylinder surface of Specimen 1

Specimen 2, while Specimen 3 is made of normalized C45. Specimen 4 consists of cast steel EN-GJS-600-3. All specimens were manufactured by turning. Mechanical and geometrical properties of the materials can be found in Table 3.

Fatigue limit experiments were carried out as stair case test according to DIN 50100 [21] for uniaxial rotary bending. Twelve specimens were used for each fatigue limit series. The experimental fatigue limit for rotary bending presented in Table 3 was determined for a survival probability of 50%. Tensile strength and Young's modulus were measured through tensile strength tests on the heat-treated material. Geometric dimensions in Table 3 represent mean values of the specimen batch used for the fatigue limit experiments.

Table 4 Surface texture parameters and roughness influence factors based on the R-profile, filtered according to setting class Sc1, for all specimens

	Specimen 1 C45 + QT	Specimen 2 42CrMo4 + QT	Specimen 3 C45 + *N*	Specimen 4 EN-GJS-600-3
Arithmetic mean height R_a [µm]	0.750	0.462	0.483	0.632
Total height, R_t [µm]	4.769	5.384	5.403	4.707
Maximum height, R_z [µm]	3.623	3.107	3.335	3.405
Mean pit depth, R_v [µm]	1.475	1.526	1.810	1.883
Roughness influence FKM, $K_{R,\sigma,FKM}$ [-]	0.9273	0.9030	0.9436	0.9578
Roughness influence Hück, $K_{R,\sigma,Hück}$ [-]	0.8921	0.8623	0.9136	0.9112
Roughness influence Liu, $K_{R,\sigma,Liu}$ [-]	0.9696	0.8797	0.9781	0.9871

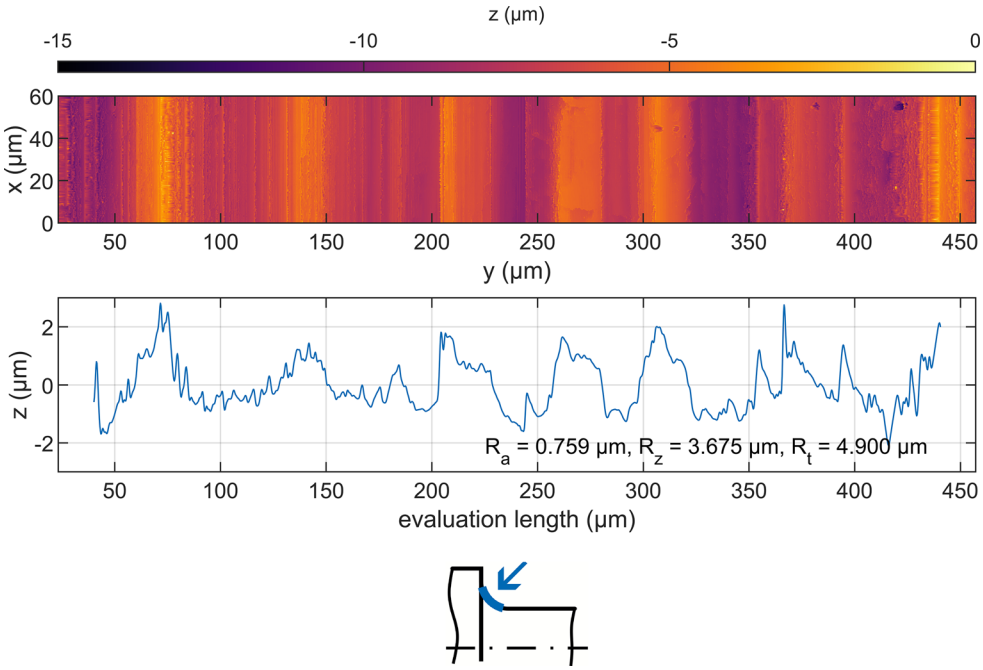

Fig. 6 Surface scan and filtered roughness profile in the notch of Specimen 1

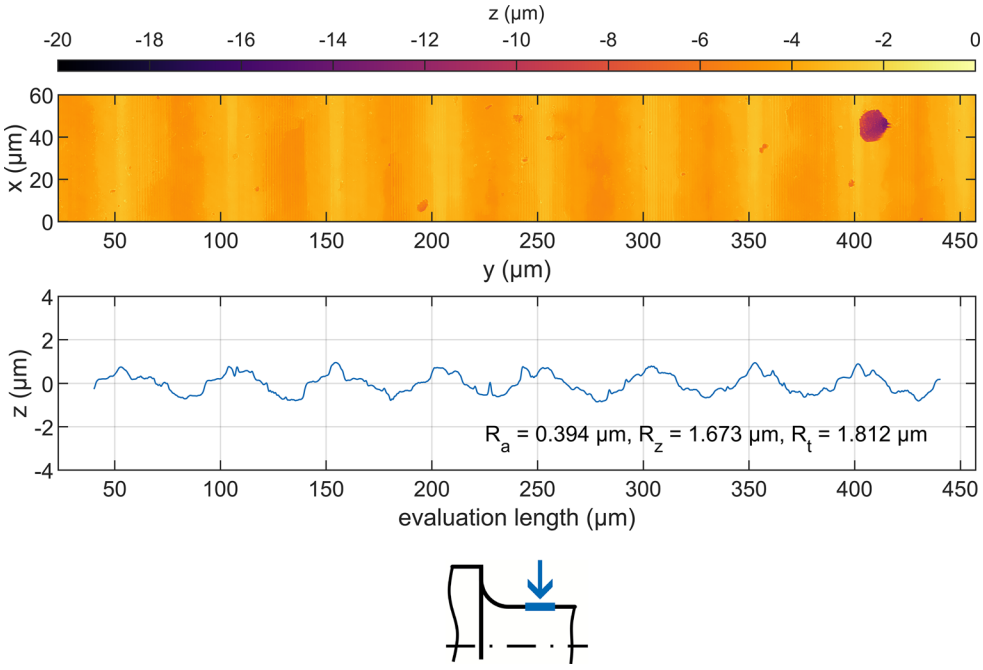

Fig. 7 Surface scan and filtered roughness profile on the cylinder surface of Specimen 2

3.1 Roughness and roughness influence factors

Impressions of all four specimen notches were taken. Afterwards, surface scans were taken on the impressions and roughness influence factors were calculated to be used recalculating the fatigue limit under rotary bending in comparison with the experiments carried out. Measurements were conducted on only one specimen per material. This is due to the fact that the sample batch was produced with a high degree of accuracy and that all the samples have similar surface characteristics, as confirmed by tactile measurements on the entire batch.

To compare surface structure, measurements on the straight cylinder surface of the impressions were also taken. Results are exemplarily shown for Specimen 1 (C45 + QT) and 2 (42CrMo4 + QT). Figures 5 and 7 depict the surface and roughness profile for the cylinder surface of the specimens and 6 and 8 show the surface and roughness profile directly at the notch of the specimens. The surface texture parameters presented in the profile plots are specific to

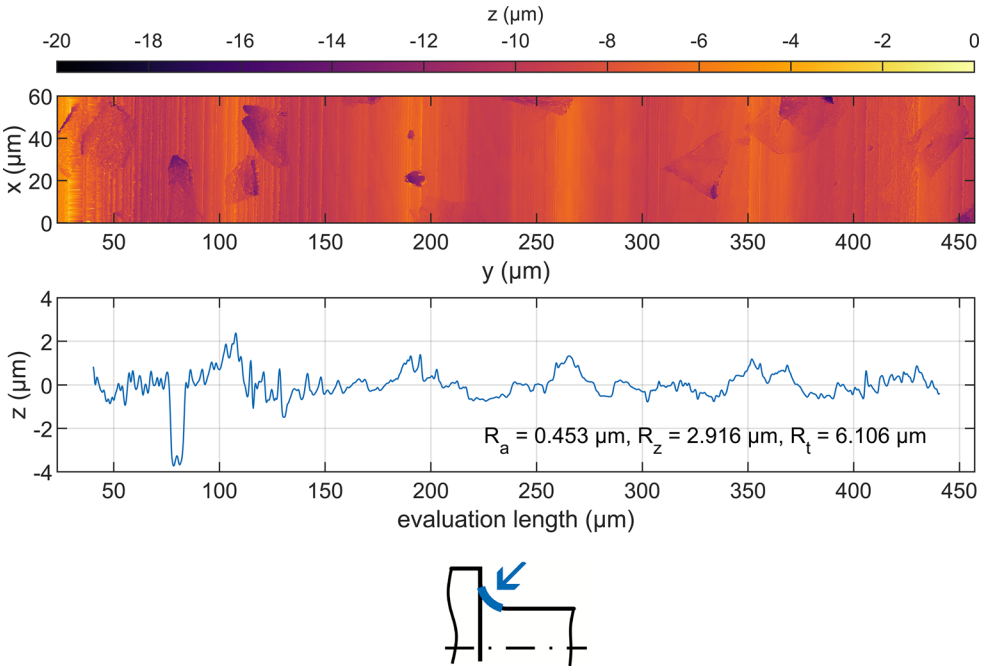

Fig. 8 Surface scan and filtered roughness profile in the notch of Specimen 2

that particular profile. Mean values for all profiles in the surface, as shown in Table 4 and 5 for the notches, are used for the recalculations.

A regular pattern can be observed in the cylinder surfaces. This is caused by the turning process used during the production of the sample. The surface at the notch shows a more irregular structure with greater height differences, which might be caused by the change of tool angle and direction relative to the specimen surface. Surface texture parameters are higher at the notch than at the cylinder surface. The other two specimens show similar behavior, the surface profile in the notch is more irregular and results in higher surface texture parameters than on the cylinder surface. These results are consistent with the findings of Becker et. al. [4].

The higher surface texture parameters lead to different surface influence factors and hence a lower predicted fatigue limit when evaluating roughness directly at the notch as opposed to the cylinder surface of the specimen.

To estimate the impact of the smaller filter nesting index in setting class Sc1, the primary profile (P-profile) is also used to calculate surface texture parameters. The P-profile contains the waviness of the surface. As only a short measurement length of 0.48 mm is used and a polynomial background is subtracted from the original surface, influence of the waviness on surface texture parameters should be minimal.

Surface texture parameters as well as roughness influence factors based on the R-profile can be found in Table 4, those based on the P-profile are shown in Table 5. As explained in Sect. 2.3, only the three empirical methods are presented here. The surface texture parameters derived from the unfiltered P-profile generally exceed those of the R-profile. The roughness influence factor developed by Liu [12] is the highest for all specimens but Specimen 2. Hence, it seems to put more weight on roughness influence for very high tensile strengths. Hück [22] consistently predicts the highest influence of surface roughness on fatigue strength.

Table 5 Surface texture parameters and roughness influence factors based on the P-profile for all specimens (K_R calculated with P-values)

	Specimen 1 C45 + QT	Specimen 2 42CrMo4 + QT	Specimen 3 C45 + *N*	Specimen 4 EN-GJS-600-3
Arithmetic mean height P_a [µm]	1.121	0.837	0.669	1.129
Total height, P_t [µm]	7.297	6.455	5.147	7.148
Maximum height, P_z [µm]	5.108	3.966	3.654	4.921
Mean pit depth, P_v [µm]	2.117	1.885	2.028	3.011
Roughness influence FKM, $K_{R,\sigma,\mathrm{FKM}}$ [-]	0.9079	0.8821	0.9393	0.9451
Roughness influence Hück, $K_{R,\sigma,\mathrm{Hück}}$ [-]	0.8646	0.8365	0.9068	0.8841
Roughness influence Liu, $K_{R,\sigma,\mathrm{Liu}}$ [-]	0.9545	0.8606	0.9791	0.9807

3.2 Fatigue limit recalculation

All recalculations in this work are based on material and specimen data obtained by measurement and given in Table 3. They are conducted for the load resulting in a nominal stress equivalent to the bending fatigue limit for a survival probability of 50%. All safety factors are set to one. Therefore, a degree of utilization of one equals a suitable prediction of the mean fatigue limit.

Two things have to be noted when evaluating the results of the fatigue limit calculation. First of all, uncertainties in other factors of the calculation can not be ruled out and influence the overall result. To evaluate on the accuracy of the different factors more specimens would be necessary but were not available for this work. To recognize the correlation between roughness and fatigue limit accurately, a broader diversification in surface roughness and manufacturing processes is required. As the specimens for this work were taken from a project not designed for roughness investigation, all specimens show similar surface texture. Secondly, only measurements suitable for setting class Sc1 of ISO 21920 [6] could be taken due to the same technological restrictions mentioned in [4]. Due to the notch radius, the sample is curved in such a way that, at a certain distance from the zero position, the critical angle resulting from the numerical aperture of the objective is exceeded and the light reflected from the surface can no longer be captured. Additionally, the LSM used has a technical limitation of 2000 z-layers, which can be quickly reached due to the inclined surface. The actual surface roughness of the parts would require setting class Sc3 to achieve valid surface texture parameters. The shorter nesting index of Sc1 results in smaller surface texture parameters compared to Sc3 which in turn lead to a potential underestimation of roughness influence on the fatigue limit. The fatigue limit is therefore calculated using both the R-profile and the P-profile.

Figure 9 summarizes the calculated degrees of utilization for all specimens using the different roughness influence factors in the FKM recalculation. As a consequence of the higher surface texture parameters resulting from the P-profile, the roughness influence factors and calculated fatigue limits are consistently lower than their counterparts based on the R-profile, leading to higher degrees of utilization. Results show, that the choice of the roughness influence factor can have a significant impact on the calculated degree of utilization. The load bearing capacity of the cast material of Specimen 4 is systematically underestimated by the FKM guideline. For the remaining samples, $K_{R,\text{Hück}}$ provides the most precise outcomes when assessing the degree of utilization. Results calculated using $K_{\text{R,Liu}}$ are least accurate. For these three specimens, fatigue limit predictions are consistently on the unsafe side with a deviation no higher than 11.3%. Since the entire recalculation was

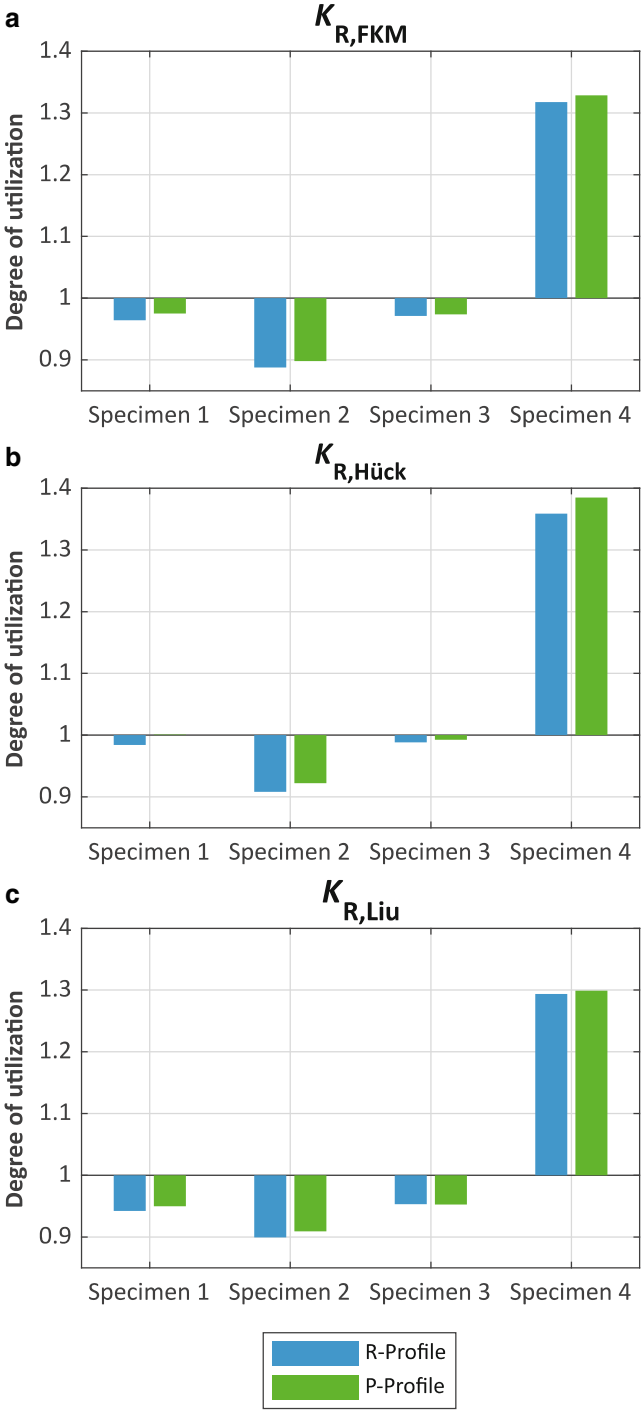

Fig. 9 Load factors for all specimens recalculated according to the FKM guideline using roughness measurements in the notch

carried out with average strength values for 50% survival probability and without any safety factor, this underestimation would be easily compensated by the basic safety factor $j_D \geq 1.2$.

Figure 10 displays the degrees of utilization calculated using surface texture parameters measured on the cylinder surface. To facilitate comparison, the degrees of utilization

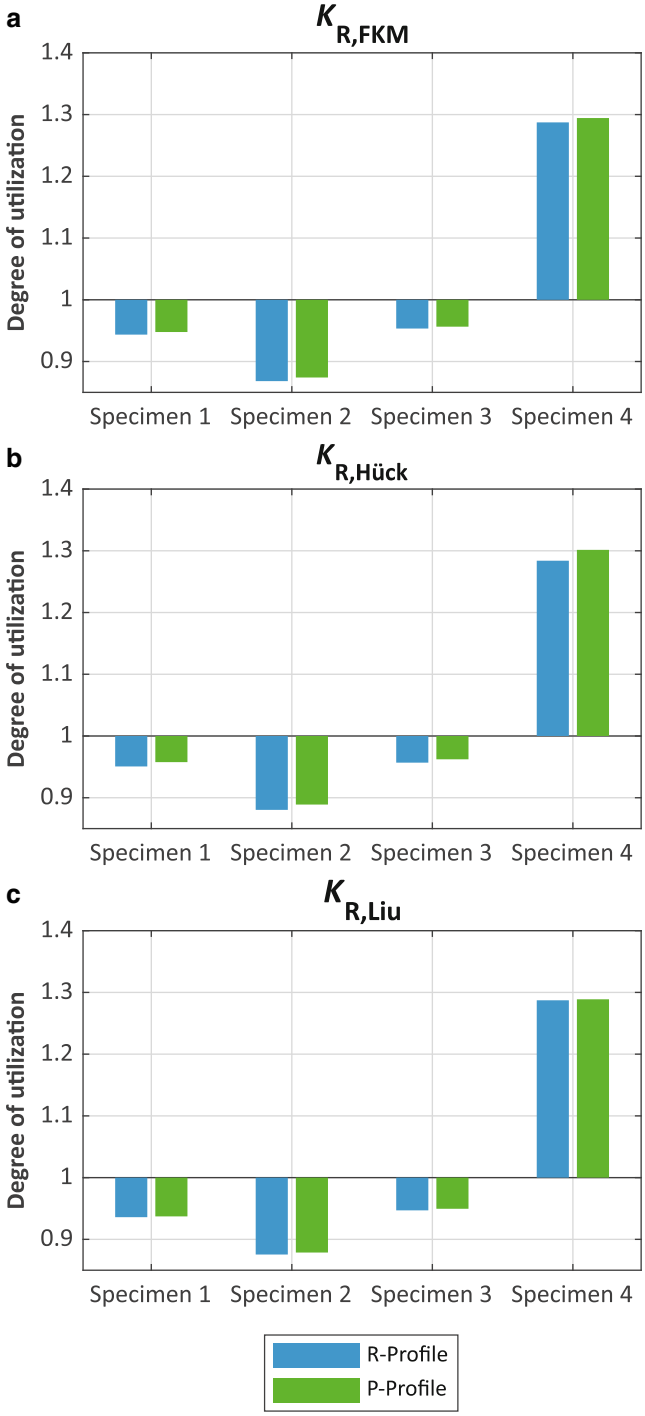

Fig. 10 Load factors for all specimens recalculated according to the FKM guideline using roughness measurements on the cylinder surface

are also evaluated with an evaluation length of 0.4 mm and setting class Sc1 for the R-values. The lower surface texture parameters result in lower calculated degrees of utilization. This general offset leads to a slightly higher accuracy for specimens 1–3 and a slightly lower accuracy for specimen 4 when using notch based surface texture parameters.

As mentioned before, it has to be considered, that only a small sample of specimens, which was not designed for systematic investigation of roughness influence on fatigue limit, was available for this work. Hence, the results only possess little statistical power to evaluate the accuracy of roughness influence factors and uncertainties in the calculation process can have significant influence on the scatter of the results. As the surface texture based roughness influence parameters take the whole evaluation length into account they probably reach limits in expressing the higher scatter in surface texture directly at the notch, leading to a general offset in surface texture parameters and degrees of utilization.

4 Conclusions

In order to determine the influence of surface roughness on the fatigue limit of steel as accurately as possible, surface roughness measurements on shaft shoulders of fatigue limit specimens were conducted. A new method using impressions of the notch surface was further refined and utilized to take measurements directly at the notch. Based on the real surface condition at the point of failure, different surface influence factors on fatigue limit were calculated.

The results indicate notable differences between the surface structure directly at the notch and on the cylinder surface of the specimens. Generally, the surface structure at the notch yields higher surface texture parameters compared to the cylinder surface. The notch surface is also more irregular, these results are consistent with previous findings by Becker et. al. [4]. In the context of the results presented, it is questionable whether current approaches to predicting the influence of roughness on fatigue limit are sufficient for the new capabilities in roughness measurement.

The ability to measure roughness directly at the point of failure should theoretically improve the quality of prediction of its influence on fatigue limit. The recalculation of the fatigue limit for four specimens in this study indicates that higher surface texture parameters in the notch result in a lower predicted fatigue limit. It is not possible to conclude whether the measurement at the notch allows for a generally more accurate prediction of the fatigue limit due to the small sample size. Since the technique for taking surface texture measurements directly at the notch is relatively new, there are no such measurements available for historic data. Generating new data, however, requires costly and time-consuming fatigue limit experiments. Hence, only the small sample presented here is currently available to compare fatigue limit calculation and experiment. One conclusion that can be drawn from the recalculation is that the choice of the roughness influence factor can significantly affect the accuracy of a specific fatigue limit prediction.

To address this issue, further research and data is required. While the measurement capabilities improve and allow for surface texture measurements directly at the point of failure of a part, the approaches to consider roughness in fatigue limit prediction reach limits in processing these measurements. The empirical factors that are widely used and based on surface texture parameters are calibrated for measurements taken away from the notch, so the different surface properties directly at the notch could lead to deviations in the prediction of roughness influence. This issue is magnified by the fact that the profiles are filtered differently due to their short length. Due to the consideration of the entire profile, it may not be possible to accurately capture the local surface texture and its higher scatter directly at the notch. As discussed in this paper, the stress concentration factor based roughness influence factors promise high accuracy due to their local approach. However, their application in fatigue limit calculation approaches seems unjustified due to the assumption of a homogeneous material and issues with the mechanical consistency of the approaches.

When using the results of the new roughness measurement method for fatigue limit calculation, users should be aware of the issues mentioned above. Until further data is available to either verify existing roughness influence parameters for notch measurements or develop new factors that are able to capture the surface texture effects in the notch, results should be used with caution and always be verified with measurements taken away from the notch.

Funding Open Access funding enabled and organized by Projekt DEAL.

Conflict of interest N. Becker, P. Tunsch, C. Ulrich and B. Schlecht declare that they have no competing interests.

References

1. Calculation of load capacity of shafts and axles—Part 1: General, DIN 743-1, Dec. 2012
2. Rennert R, Kullig E, Vormwald M, Esderts A, Luke M (2020) Analytical strength assessment of components: made of steel, cast iron and aluminium materials: FKM guideline, 7th edn. VDMA Verlag GmbH, Frankfurt am Main
3. Siebel G, Gaier M (1956) Untersuchungen über den Einfluss der Oberflächenbeschaffenheit auf die Dauerschwingfestigkeit metallischer Bauteile. VDI-Z 98(30):1715–1723
4. Becker N, Ulrich C, Körner C, Schlecht B (2023) A novel method for measurements of surface topography in previously inaccessible areas. Mater Test. https://doi.org/10.1515/mt-2023-0269 (Electronically published ahead of print)
5. Jerome WG, Price RL (eds) (2018) Basic Confocal Microscopy. Springer, Cham https://doi.org/10.1007/978-3-319-97454-5
6. Geometrical product specifications (GPS) (2021) Surface texture: Profile—Part 2: Terms, definitions and surface texture parameters. ISO, Dec, pp 21920–21922
7. Accessed RPTB https://www.ptb.de/rptb. Accessed 26 Jan 2023
8. Arola D, Williams C (2002) Estimating the fatigue stress concentration factor of machined surfaces. Int J Fatigue 24(9):923–930. https://doi.org/10.1016/S0142-1123(02)00012-9
9. (2012) Calculation of load capacity of shafts and axles. In: Part 2: Theoretical stress concentration factors and fatigue notch factors. DIN, pp 743–742
10. Gudehus H, Zenner H (1995) Leitfaden für eine Betriebsfestigkeitsrechnung, 3rd edn. Verlag Stahleisen, Düsseldorf
11. Hück M, Thrainer L, Schütz W (1981) Berechnung von Wöhlerlinien für Bauteile aus Stahl, Stahlguß und Grauguß: Synthet. Wöhlerlinien. In: Arbeitsgemeinschaft Betriebsfestigkeit: Bericht der Arbeitsgemeinschaft Betriebsfestigkeit, vol 11. Stahleisen, Düsseldorf
12. Liu J (2001) Dauerfestigkeitsberechnung metallischer Bauteile, 1st edn. Papierflieger, Clausthal-Zellerfeld (http://slubdd.de/katalog?TN_libero_mab2)
13. Pilkey WD, Pilkey DF, Bi Z (2020) Peterson's Stress Concentration Factors. Wiley, Online (Available: https://books.google.de/books?id=apXFDwAAQBAJ)
14. Neuber (1958) Kerbspannungslehre
15. Arola D, Ramulu M (1999) An Examination of the Effects from Surface Texture on the Strength of Fiber Reinforced Plastics. J Compos Mater 33(2):102–123. https://doi.org/10.1177/002199839903300201
16. Vetter S, Leidich E, Becker N, Schlecht B, Hasse A (2022) Probabilistic Method to Estimate the Scatter of the Fatigue Strength of Shafts in the HCF Region. In: Procedia Structural Integrity, pp 746–754
17. Vetter S (2023) Abschätzung der Streuung der Schwingfestigkeit von Wellen und Achsen im Bereich der Langzeitfestigkeit. Dissertation, Technische Universität Chemnitz, Chemnitz
18. Weibull W (1949) A statistical representation of fatigue failures in solids. In: Transactions of the royal institute of technology Stockholm, vol 27. Sweden
19. Böhm J, Heckel K (1982) Die Vorhersage der Dauerschwingfestigkeit unter Berücksichtigung des statistischen Größeneinflusses. Mat-wiss U Werkstofftech 13(4):120–128. https://doi.org/10.1002/mawe.19820130408
20. Tunsch P (2023) Bewertung des Rauheitseinflusses auf die Tragfähigkeit von Wellenabsätzen, Diplomarbeit, Technische Universität Dresden. Dresden, Dresden
21. Load controlled fatigue testing—Execution and evaluation of cyclic tests at constant load amplitudes on metallic specimens and components, DIN 50100, Dec. 2022
22. Gudehus H, Zenner H (1995) Leitfaden für eine Betriebsfestigkeitsrechnung, 3rd edn. Verlag Stahleisen, Düsseldorf